

The I-Love universal relation for polytropic stars under Newtonian gravity

Rui Xu,^{1,*} Alejandro Torres-Orjuela,² Lars Andersson,² and Pau Amaro Seoane³

¹*Department of Astronomy, Tsinghua University, Beijing 100084, China*

²*Beijing Institute of Mathematical Sciences and Applications, Beijing 101408, China*

³*Institute for Multidisciplinary Mathematics, Polytechnic University of València, València 46022, Spain*

(Dated: January 14, 2025)

The moment of inertia and tidal deformability of idealized stars with polytropic equations of state (EOSs) are numerically calculated under both Newtonian gravity and general relativity (GR). The results explicitly confirm that the relation between the moment of inertia and tidal deformability, parameterized by the star's mass, exhibits variations of 1% to 10% for different polytropic indices in Newtonian gravity and GR, respectively. This indicates a more robust I-Love universal relation in the Newtonian framework. The theoretically derived I-Love universal relation for polytropic stars is subsequently tested against observational data for the moment of inertia and tidal deformability of the 8 planets and some moons in our solar system. The analysis reveals that the theoretical I-Love universal relation aligns well with the observational data, suggesting that it can serve as an empirical relation. Consequently, it enables the estimation of either the moment of inertia or the tidal deformability of an exoplanet if one of these quantities, along with the mass of the exoplanet, is known.

I. INTRODUCTION

The universal relations for neutron stars (NSs) and quark stars (QSs) were first identified by Yagi and Yunes in terms of the moment of inertia (I), tidal deformability (Love), and quadrupole moment (Q) of these compact stars [1, 2]. These relations, known as I-Love-Q universal relations, are termed “universal” because they exhibit remarkable insensitivity to the equation of state (EOS) of the compact object. Even for EOSs that produce significantly different mass-radius relations for NSs and QSs, the I-Love-Q relations hold with a precision better than 1%. Subsequently, the universal relations were extended to include additional perturbative properties of compact stars, such as higher-order multipolar tidal deformabilities [3–7] and oscillation mode frequencies [8–10]. While these extended universal relations are valuable, their precision is generally lower than that of the original I-Love-Q relations, with discrepancies reaching up to 10% for different EOSs [11].

The precise mechanism underlying the universality of these relations remains unclear. Unlike the no-hair theorem for black holes in general relativity (GR) [12], the I-Love-Q universal relations are not exact and are established through numerical studies. Their accuracy often deteriorates when simplifying assumptions used in structural and perturbative calculations of stars are relaxed [13, 14]. For instance, factors such as anisotropic pressure, non-barotropic EOSs, or the inclusion of more complex physics introduce greater discrepancies in the universal relations [7, 15–20]. Moreover, the validity of the universal relations can also depend on the gravitational theory. While the I-Love universal relation has been shown to hold in many scalar-tensor theories (albeit with up to 10% discrepancies) [21–23], it is visibly broken in specific scalar-tensor theories where the Gauss-Bonnet invariant is coupled to the square of a scalar field [24]. In such cases, the Schwarzschild solution is no longer unique, and scalar-

ized black holes appear, violating the no-hair theorem [25–27]. Whether a connection exists between the breakdown of the I-Love universal relation and the violation of the no-hair theorem warrants further investigation.

Although the universal relations for NSs and QSs are widely studied because they mitigate EOS-related ambiguities in compact star studies, they are not exclusive to compact stars. As shown analytically in Ref. [2] using two specific polytropic EOSs, the I-Love-Q universal relations also apply to spherical objects in the Newtonian limit. This work explicitly confirms the I-Love universal relation for general polytropic EOSs in Newtonian gravity and compares it with the corresponding relation in GR. A noteworthy application of the I-Love universal relation for polytropic EOSs in Newtonian gravity is its use in analyzing the tidal Love number and moment of inertia of solar-system planets and their moons. Despite their layered structures and complex compositions, which deviate from simple polytropic EOSs, these celestial objects conform well to the I-Love universal relation. This finding highlights the potential of the I-Love relation as a powerful tool not only for studying compact stars but also for deducing properties of exoplanets.

We begin by reviewing the formulae used to calculate the tidal deformability and the moment of inertia in Newtonian gravity in Sec. II A, and in general relativity (GR) in Sec. II B. In Sec. II C, we present numerical results for polytropic EOSs. In Sec. II D, we list and plot measurements of the tidal Love number and the moment of inertia for 17 planets and moons, comparing them with the I-Love universal relation for polytropic stars. A brief summary is provided in Sec. III.

It is worth noting that the I-Love relation for white dwarfs deviates slightly from the I-Love universal relations in both Newtonian gravity and GR. The relevant results are included in Appendix A. Throughout this work, geometrized units are used, where the gravitational constant G and the speed of light c are set to one. SI units are also employed to express the values of physical quantities. The metric sign convention used is $(-, +, +, +)$.

* Corresponding author: xuru@tsinghua.edu.cn

II. I-LOVE UNIVERSAL RELATIONS FOR POLYTROPIC STARS

A. Newtonian gravity

A comprehensive account of the spherically hydrostatic stars with polytropic EOSs and their perturbations can be found in Ref. [28]. We briefly review the formulae here. First, the basic set of equations consists of the Poisson's equation and the energy-momentum conservation equations,

$$\begin{aligned}\nabla^2\Phi &= -4\pi\rho, \\ \frac{\partial\rho}{\partial t} + \nabla \cdot (\rho\mathbf{v}) &= 0, \\ \frac{\partial\mathbf{v}}{\partial t} + (\mathbf{v} \cdot \nabla)\mathbf{v} &= \nabla\Phi - \frac{1}{\rho}\nabla p,\end{aligned}\quad (1)$$

where Φ is the Newtonian potential, and ρ , p , \mathbf{v} are the density, the pressure, and the velocity of the fluid constituting the star. Then, the variables assume the form

$$\begin{aligned}\Phi &= \Phi^{(0)} + \delta\Phi, \\ \rho &= \rho^{(0)} + \delta\rho, \\ p &= p^{(0)} + \delta p, \\ \mathbf{v} &= \mathbf{v}^{(0)} + \delta\mathbf{v}.\end{aligned}\quad (2)$$

The zeroth-order terms correspond to the spherically symmetric hydrostatic solution, while the perturbation terms account for the tidal perturbation under consideration. If one assumes that the zeroth-order terms of the variables depend only on the radial coordinate r , with $\mathbf{v}^{(0)} = 0$, the hydrostatic equations for spherical Newtonian stars are obtained:

$$\begin{aligned}\Phi^{(0)''} + \frac{2}{r}\Phi^{(0)'} &= -4\pi\rho, \\ p^{(0)'} &= \rho^{(0)}\Phi^{(0)'},\end{aligned}\quad (3)$$

where the prime denotes the derivative with respect to r .

For the perturbation of Eq. (1), it is convenient to use the Lagrangian displacement $\boldsymbol{\xi}$ of the perturbed fluid elements. Without considering the uninteresting odd-parity perturbations, $\boldsymbol{\xi}$ can be expressed in terms of the even-parity spherical harmonics,

$$\boldsymbol{\xi} = (\mathbf{d}rW_1 + \mathbf{d}\theta V\partial_\theta + \mathbf{d}\phi V\partial_\phi)Y_{lm},\quad (4)$$

where $\{\mathbf{d}r, \mathbf{d}\theta, \mathbf{d}\phi\}$ is the basis for covariant components of vectors and tensors in the spherical coordinates (r, θ, ϕ) , W_1 and V are functions depending on r only, and Y_{lm} are the usual spherical harmonics. Note that $(\mathbf{d}\theta\partial_\theta + \mathbf{d}\phi\partial_\phi)Y_{lm}$ comes from the even-parity vector spherical harmonics [29]

$$\begin{aligned}\mathbf{Y}_{lm}^E &:= \frac{r}{\sqrt{l(l+1)}}\nabla Y_{lm} \\ &= \frac{r}{\sqrt{l(l+1)}}(\mathbf{d}\theta\partial_\theta + \mathbf{d}\phi\partial_\phi)Y_{lm}.\end{aligned}\quad (5)$$

Using $\boldsymbol{\xi}$, the perturbations of the density, the pressure, and the velocity are

$$\delta\rho = -\rho\nabla \cdot \boldsymbol{\xi} - (\boldsymbol{\xi} \cdot \nabla)\rho,$$

$$\begin{aligned}\delta p &= -\Gamma_1 p \nabla \cdot \boldsymbol{\xi} - (\boldsymbol{\xi} \cdot \nabla)p, \\ \delta\mathbf{v} &= \partial_t \boldsymbol{\xi} + (\mathbf{v} \cdot \nabla)\boldsymbol{\xi} - (\boldsymbol{\xi} \cdot \nabla)\mathbf{v},\end{aligned}\quad (6)$$

where Γ_1 is the adiabatic index for fluid elements under the perturbations. For barotropic EOSs where p depends solely on ρ , one has

$$\Gamma_1 = \frac{\rho}{p} \frac{dp}{d\rho}.\quad (7)$$

Especially, for the polytropic EOSs

$$p = \alpha\rho^{1+\frac{1}{n}},\quad (8)$$

where α and n are constants, we have $\Gamma_1 = 1 + 1/n$ with n being the polytropic index.

Using Eq. (4) and Eq. (6) to write out the linear order of Eq. (1), one finds that the variables W_1 and V can be expressed in terms of $\delta\Phi$, so that there is only one ordinary differential equation (ODE) for $\delta\Phi$ to be solved:

$$\delta\Phi'' + \frac{2}{r}\delta\Phi' + \left(4\pi\rho\frac{\rho'}{\rho} - \frac{l(l+1)}{r^2}\right)\delta\Phi = 0.\quad (9)$$

Note that Eq. (9) is supposed to be valid at the linear order, so ρ , p and their radial derivatives take the zeroth order values. Equation (9) has the simple solution $C_l r^l + D_l r^{-l-1}$ outside the star, where C_l and D_l are constants. Interpreting the r^l terms as an external tidal field and the r^{-l-1} terms as the multipolar response of the star to the external tidal field, the tidal Love numbers are defined as

$$k_l := \frac{1}{2} \frac{1}{R^{2l+1}} \frac{D_l}{C_l},\quad (10)$$

where R is the radius of the star. Focusing on the lowest tidal term which is proportional to r^2 , it causes a quadrupole term as the response, namely that it is the $l = 2$ case. In this case, the tidal deformability is defined as

$$\lambda_2 := \frac{1}{3} \frac{D_2}{C_2} = \frac{2k_2}{3} R^5.\quad (11)$$

The fluid variables and the Newtonian potential need to be finite at the center of the star. This turns out to be a condition that fixes the ratios between C_l and D_l , so that k_l can be calculated uniquely given a solution of $\delta\Phi$ inside the star. In fact, an expansion analysis of Eq. (3) and Eq. (9) leads to

$$\begin{aligned}\Phi^{(0)'} &\approx -\frac{4\pi}{3}r\rho_0, \\ p^{(0)} &\approx p_0, \\ \delta\Phi &\approx A_l r^l,\end{aligned}\quad (12)$$

at $r \rightarrow 0$, where ρ_0 and p_0 are the density and the pressure at the center of the star, and A_l are constants that simply scale the solution of $\delta\Phi$. For a given EOS, ρ_0 and p_0 are related. Therefore the solutions to Eq. (3) and Eq. (9) are controlled by one free parameter.

Given a barotropic EOS, one can numerically integrate Eq. (3) and Eq. (9) from a tiny r where the approximation

in Eq. (12) is valid to a radius where p vanishes to obtain the solution inside the star. By matching $\delta\Phi$ and $\delta\Phi'$ at the surface of the star to the exterior solution $C_l r^l + D_l r^{-l-1}$, C_l and D_l can be determined so that k_l can be calculated. As for the moment of inertia, it is obtained simply through the integral

$$I = \int (r \sin \theta)^2 \rho^{(0)} d^3 x. \quad (13)$$

B. General relativity

The perturbation theory in GR to calculate the moment of inertia and the tidal deformability of a static spherical star is well-established in the literature; e.g., see Refs. [30–33]. To compare with the formulae in Newtonian gravity parallelly, we briefly review the GR counterpart.

The basic equations to start with are the Einstein field equations

$$G_{\mu\nu} = 8\pi T_{\mu\nu}, \quad (14)$$

with the energy-momentum tensor of the fluid

$$T_{\mu\nu} = (\epsilon + p) u_\mu u_\nu + p g_{\mu\nu}, \quad (15)$$

where ϵ , p and u_μ are the proper energy density, the proper pressure, and the four-velocity of the fluid elements. The energy-momentum conservation equation $D^\mu T_{\mu\nu} = 0$, where D_μ is the covariant derivative, is a consequence of the Einstein field equations. The variables are set up to be the static spherical background configuration plus perturbations, namely

$$\begin{aligned} g_{\mu\nu} &= g_{\mu\nu}^{(0)} + \delta g_{\mu\nu}, \\ \epsilon &= \epsilon^{(0)} + \delta\epsilon, \\ p &= p^{(0)} + \delta p, \\ u_\mu &= u_\mu^{(0)} + \delta u_\mu. \end{aligned} \quad (16)$$

Using the spherical ansatz

$$g_{\mu\nu}^{(0)} dx^\mu dx^\nu = g_{tt}^{(0)} dt^2 + \left(1 - \frac{2m}{r}\right)^{-1} dr^2 + r^2 d\Omega^2, \quad (17)$$

for the background metric, one obtains from the Einstein field equations the Tolman-Oppenheimer-Volkoff (TOV) equation

$$\begin{aligned} m' &= 4\pi r^2 \epsilon^{(0)}, \\ p^{(0)'} &= -(\epsilon^{(0)} + p^{(0)}) \frac{m + 4\pi r^3 p^{(0)}}{r(r - 2m)}, \end{aligned} \quad (18)$$

where the prime denotes the derivative with respect to r .

The perturbations are decomposed into spherical harmonic modes to naturally satisfy the angular dependence in the Einstein field equations. In addition to the even-parity vector spherical harmonics in Eq. (5), we also need the odd-parity vector spherical harmonics [29]

$$\mathbf{Y}_{lm}^B := \frac{1}{\sqrt{l(l+1)}} \mathbf{r} \times \nabla Y_{lm}$$

$$= \frac{r}{\sqrt{l(l+1)}} \left(-\frac{d\theta}{\sin\theta} \partial_\phi + d\phi \sin\theta \partial_\theta \right) Y_{lm}. \quad (19)$$

In the Regge-Wheeler gauge [34], the even-parity perturbations of the metric are

$$\delta g_{\mu\nu} = e^{i\sigma t} \begin{pmatrix} -g_{tt}^{(0)} H_0 & H_1 & 0 & 0 \\ \text{sym} & g_{rr}^{(0)} H_2 & 0 & 0 \\ 0 & 0 & r^2 K & 0 \\ 0 & 0 & 0 & r^2 \sin^2 \theta K \end{pmatrix} Y_{lm}, \quad (20)$$

while the odd-parity perturbations of the metric are

$$\delta g_{\mu\nu} = e^{i\sigma t} \begin{pmatrix} 0 & 0 & -h_0 \frac{1}{\sin\theta} \partial_\phi & h_0 \sin\theta \partial_\theta \\ \text{sym} & 0 & -h_1 \frac{1}{\sin\theta} \partial_\phi & h_1 \sin\theta \partial_\theta \\ \text{sym} & \text{sym} & 0 & 0 \\ \text{sym} & \text{sym} & \text{sym} & 0 \end{pmatrix} Y_{lm}, \quad (21)$$

where H_0 , H_1 , H_2 , K and h_0 , h_1 are functions of r , and σ is the oscillation frequency of the mode. The perturbations corresponding to a static tidal field and a slowly rigid rotation are time-independent, so the limit $\sigma \rightarrow 0$ is taken once the equations for the perturbation variables are obtained. The symbol ‘‘sym’’ means the symmetric property $\delta g_{\mu\nu} = \delta g_{\nu\mu}$.

For the perturbations in the fluid sector, the fundamental variable is the Lagrangian displacement ξ_μ for the perturbed fluid elements. It takes the form

$$\xi_\mu = e^{i\sigma t} (W_0, W_1, V \partial_\theta, V \partial_\phi) Y_{lm}, \quad (22)$$

for the even parity, and

$$\xi_\mu = e^{i\sigma t} \left(0, 0, -U \frac{1}{\sin\theta} \partial_\phi, U \sin\theta \partial_\theta \right) Y_{lm}, \quad (23)$$

for the odd parity, where W_0 , W_1 , V and U are functions of r . The perturbations of the energy density, the pressure, and the four-velocity can be expressed in terms of $\delta g_{\mu\nu}$ and ξ_μ via [35]

$$\begin{aligned} \Delta\epsilon &= -\frac{1}{2} (\epsilon + p) (g^{\mu\nu} + u^\mu u^\nu) \Delta g_{\mu\nu}, \\ \Delta p &= -\frac{1}{2} \Gamma_1 p (g^{\mu\nu} + u^\mu u^\nu) \Delta g_{\mu\nu}, \\ \Delta u^\mu &= \frac{1}{2} u^\mu u^\alpha u^\beta \Delta g_{\alpha\beta}. \end{aligned} \quad (24)$$

Note that those are Lagrangian perturbations. The Eulerian perturbations that are directly used in the Einstein field equations can be obtained via $\Delta = \delta + \mathcal{L}_\xi$, where \mathcal{L}_ξ is the Lie derivative along the vector ξ_μ . For example,

$$\mathcal{L}_\xi u^\mu = \xi^\alpha D_\alpha u^\mu - u^\alpha D_\alpha \xi^\mu. \quad (25)$$

In Eq. (24), we have used

$$\Gamma_1 = \frac{\epsilon + p}{p} \frac{dp}{d\epsilon}, \quad (26)$$

which is the relativistic version of the adiabatic index for fluid elements under the perturbations. We take

$$p = \alpha \epsilon^{1+\frac{1}{n}} \quad (27)$$

as the relativistic version of the polytropic EOSs, so $\Gamma_1 = (1 + p/\epsilon)(1 + 1/n)$ in this case.

Substituting the perturbations of the metric and the perturbations in the fluid sector into the Einstein field equations and the energy-momentum conservation equation, one obtains

$$\begin{aligned}
H_0'' + \frac{2(r-m) - 4\pi r^3(\epsilon - p)}{r(r-2m)} H_0' - \frac{l(l+1)m}{r(r-2m)(m+4\pi r^3 p)} H_0 - \frac{4m^3}{r^2(r-2m)^2(m+4\pi r^3 p)} H_0 \\
- \frac{4\pi r^3 (r\epsilon' + l(l+1)p + 64\pi^2 r^4 p^3 - 20\pi r^2 \epsilon p - 36\pi r^2 p^2)}{(r-2m)^2(m+4\pi r^3 p)} H_0 \\
- \frac{4\pi r^2 m (40\pi r^2 \epsilon p + 120\pi r^2 p^2 - 5\epsilon - (2l^2 + 2l + 9)p - 4r\epsilon') + 8\pi r m^2 (2r\epsilon' + 5\epsilon + 15p)}{(r-2m)^2(m+4\pi r^3 p)} H_0 = 0.
\end{aligned} \tag{28}$$

The physical solution behaves as

$$H_0 \approx A_l r^l, \tag{29}$$

at the center of the star, and

$$H_0 \approx C_l r^l + D_l r^{-l-1}, \tag{30}$$

at infinity. By numerically solving Eq. (28) from the center of the star to a large enough radius, one can extract C_l and D_l from the solution, and hence calculate the tidal Love numbers using the same definition as in Eq. (10) and the tidal deformability using the same definition as in Eq. (11).

The odd-parity perturbation equations are much simpler than the even ones. In fact, the equation for the fluid variable U is algebraic. For the time-independent case, we have

$$U \rightarrow \frac{i}{\sigma} \sqrt{\frac{4\pi}{3}} \tilde{\Omega} r^2, \tag{31}$$

where $\tilde{\Omega}$ is a constant, at the limit $\sigma \rightarrow 0$, so that the angular velocity of the star is

$$\Omega = \sqrt{\frac{2l+1}{3}} \tilde{\Omega} \frac{d}{d \cos \theta} P_l(\cos \theta). \tag{32}$$

The rotation of the star is rigid for $l = 1$ and differential for $l \geq 2$. The equation for h_0 in the time-independent case is

$$\begin{aligned}
h_0'' - \frac{8\pi r^2(\epsilon + p)}{2(r-2m)} h_0' - \frac{8\pi r^3(\epsilon + p) + l(l+1)r - 4m}{r^2(r-2m)} h_0 \\
+ \frac{\sqrt{\frac{\pi}{3}} 32\pi r^3(\epsilon + p)}{r-2m} \tilde{\Omega} = 0.
\end{aligned} \tag{33}$$

At the center of the star, the physical solution behaves as

$$h_0 \approx a_l r^{l+1} + h_{0\text{in}}, \tag{34}$$

where a_l are constants, and $h_{0\text{in}}$ is a particular solution to Eq. (33) and proportional to the constant $\tilde{\Omega}$. At infinity, the physical solution behaves as

$$h_0 \approx d_l r^{-l}, \tag{35}$$

ODEs for the variables $H_0, H_1, H_2, K, h_0, h_1$ and W_1, V, U . We focus on the time-independent case to calculate the tidal deformability with the $l = 2$ even-parity perturbation and the moment of inertia with the $l = 1$ odd-parity perturbation.

With $\sigma = 0$, the even-parity perturbation equations can be simplified to a single second-order ODE for H_0 ,

where d_l are constants. Numerical integrations start near $r = 0$ where Eq. (34) is valid. By setting $a_l = 1$ and adjusting $\tilde{\Omega}$ to a suitable value, the asymptotic behavior in Eq. (35) can be achieved. Especially, for $l = 1$, the asymptotic behavior in Eq. (35) means that the metric component $g_{t\phi}$ behaves as

$$g_{t\phi} \approx -\frac{2J}{r} \sin^2 \theta, \tag{36}$$

at infinity, where $J = \sqrt{3} d_1 / \sqrt{16\pi}$ is the angular momentum of the spacetime. Therefore, the moment of inertia can be calculated via

$$I = \frac{J}{\tilde{\Omega}} = \sqrt{\frac{3}{16\pi}} \frac{d_1}{\tilde{\Omega}}, \tag{37}$$

once d_1 and $\tilde{\Omega}$ are known.

In practice, there is a trick to solve Eq. (33) for $l = 1$ only. A change of variable

$$h_0 = -\sqrt{\frac{4\pi}{3}} r^2 (\omega - \tilde{\Omega}), \tag{38}$$

simplifies Eq. (33) to a homogeneous equation of ω for $l = 1$. And outside the star, ω has the simple solution

$$\omega = c + \frac{d}{r^3}, \tag{39}$$

where c and d are constants. For h_0 and $g_{t\phi}$ to have the correct asymptotic behavior, one finds

$$\begin{aligned}
c &= \tilde{\Omega}, \\
d &= -2J.
\end{aligned} \tag{40}$$

Therefore, by numerically solving ω inside the star and matching ω and ω' at the surface of the star, one obtains c and d , and hence $I = -d/(2c)$.

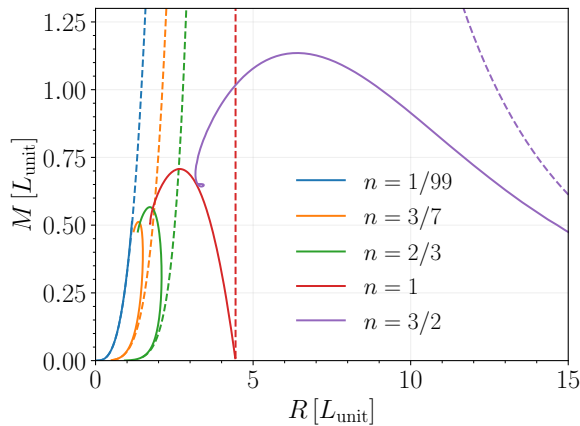


FIG. 1. The mass-radius relation for polytropic stars. The dashed lines are the Newtonian results, and the solid lines are the results using GR. Notice that the Newtonian lines extend to infinite mass.

C. Numerical results

Using the above formulae, we calculate the $l = 2$ tidal deformability and the moment of inertia for polytropic stars in both Newtonian gravity and GR.

First, as a preparation for calculating the tidal deformability and the moment of inertia, masses and radii of the background spherical stars are calculated using polytropic EOSs with different values of indices. Figure 1 presents the results. The following length parameter has been used as the unit of the mass and radius of the polytropic stars:

$$L_{\text{unit}} = \frac{1}{\sqrt{4\pi}} \alpha^{n/2}, \quad (41)$$

where α is the dimensional coefficient, and n is the polytropic index in Eq. (8) for Newtonian gravity and Eq. (27) for GR.

One observation from Fig. 1 merits addressing: the Newtonian mass-radius relations extend indefinitely as the central density and pressure approach infinity, meaning there is no maximal mass for Newtonian stars with polytropic EOSs, while the mass-radius relations in GR have maximal masses which mark critical points where the solutions start to be unstable. Note that in the following Figs. 2-5, the GR results have been truncated at the maximal-mass points and the unstable solutions are not shown for the clearness of the plots.

Then, in Fig. 2, results of the moment of inertia and the tidal deformability are converted to the moment of inertia factor $I/(MR^2)$ and the tidal Love number k_2 , and plotted against the mass of the star. We point out that for a given polytropic index n , the moment of inertia factor $I/(MR^2)$ and the tidal Love number k_2 remarkably remain constant as the mass of the Newtonian star varies.

Finally, in Fig. 3, the moment of inertia I and the tidal deformability λ_2 , both parameterized by the mass of the star, are plotted. It is evident that different polytropic indices result in universal relations between I/M^3 and λ_2/M^5 in Newtonian gravity and GR separately. While the universal relation in Newtonian gravity meets the universal relation in GR at the

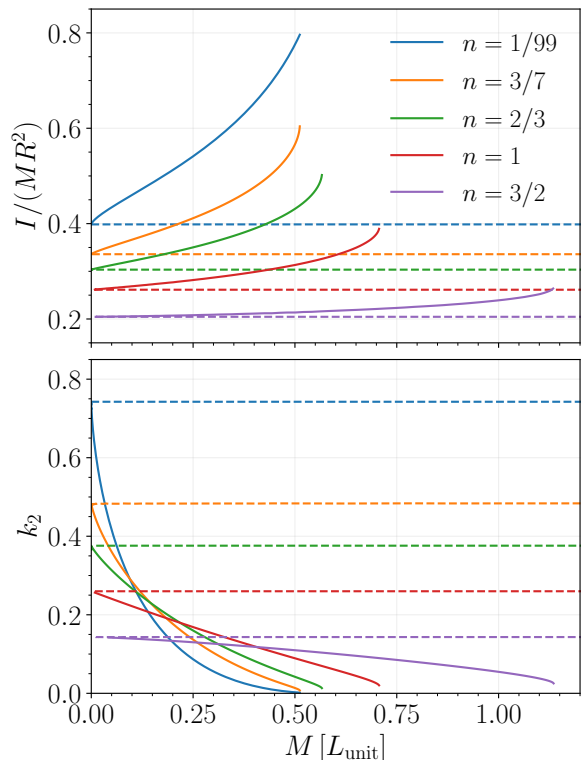


FIG. 2. Upper panel: the moment of inertia factor $I/(MR^2)$ versus the mass of the polytropic star. Lower panel: the tidal Love number k_2 versus the mass of the polytropic star. The dashed lines are the Newtonian results, and the solid lines are the results using GR. Notice that the Newtonian results do not change with the mass of the star.

higher end of λ_2/M^5 , which is the regime of the Newtonian limit, they deviate from each other at the lower end of λ_2/M^5 , corresponding to large masses and compact stars. The deviations between results for different n are smaller in Newtonian gravity than in GR, indicating that the universality of the relation holds more robustly in Newtonian gravity.

To assess the applicability of the polytropic EOS results to real stars, we also calculated λ_2 and I for NSs using the tabulated EOS SLy4 [36, 37] and for white dwarfs using the theoretical EOS under the zero-temperature approximation (see Appendix A). For NSs, the I/M^3 versus λ_2/M^5 relation derived from EOS SLy4 aligns well with the universal relation for polytropic EOSs. For white dwarfs, there is a discrepancy of about 10% between their I/M^3 versus λ_2/M^5 relation and the universal relation in GR. Notably, λ_2 and I for white dwarfs were calculated within the GR framework, so their I/M^3 versus λ_2/M^5 relation is compared with the universal relation in GR, even though Fig. 3 shows that the line for white dwarfs is closer to the Newtonian line.

We note the analytical form of the universal relation in Newtonian gravity, obtained from the special case $n \rightarrow 0$. When $n \rightarrow 0$, the polytropic EOS describes stars with uniform density, allowing analytical solutions for Eq. (3) and Eq. (9). Considering the density discontinuity at the star's surface, one

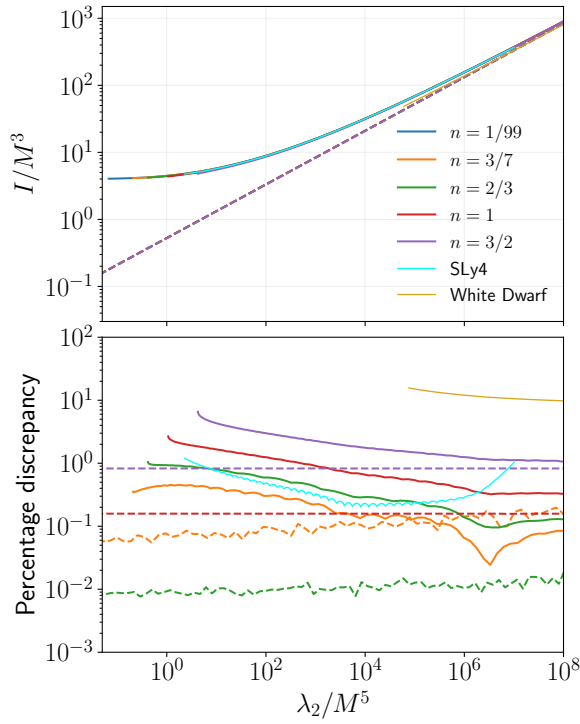


FIG. 3. Upper panel: the I-Love universal relation in Newtonian gravity (dashed lines) and in GR (solid lines). Lower panel: Relative discrepancies between each line and the $n = 1/99$ lines in Newtonian gravity and in GR, correspondingly. The results using the SLy4 EOS, which is a realistic EOS for NSs, and the zero-temperature EOS for white dwarfs are also plotted for comparison.

finds $k_2 = 3/4$ [28]. Additionally, $I/(MR^2) = 2/5$ is known for a spherical star with uniform density. Therefore, in this case, we obtain

$$\frac{I}{M^3} = \frac{2^{7/5}}{5} \left(\frac{\lambda_2}{M^5} \right)^{2/5}. \quad (42)$$

Let us address that the I-Love universal relation is completely nontrivial before we turn to its application. For demonstration, we plot in Fig. 4 I/R^3 versus λ_2/R^5 where I and λ_2 are parameterized using the radius R rather than the mass M , and in Fig. 5 the compactness $C := M/R$ versus λ_2/M^5 . Neither of them is universal. The miraculous I-Love universal relation holds between I and λ_2 , specifically parameterized by the mass of the star, not between any other seemingly plausible quantities.

D. Checking against the planets in the solar system

For NSs, verifying the I-Love universal relation through measurements remains challenging due to the lack of simultaneous observations of I and λ_2 . However, for Newtonian stars, the I-Love universal relation can be validated using measurements from planets and moons within our solar system. Table I provides the masses, radii, moment of inertia factors, and

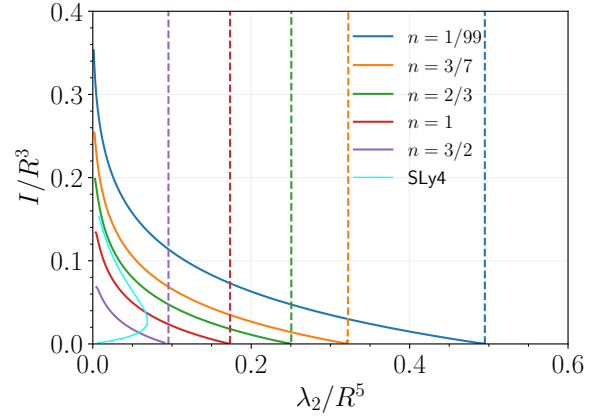


FIG. 4. An example of non-universal relation: I/R^3 versus λ_2/R^5 . The dashed lines are the Newtonian results, and the solid lines are the results using GR. The result of NSs (SLy4) is also plotted for comparison. The result of white dwarfs has too small values of I/R^3 to show in the plot.

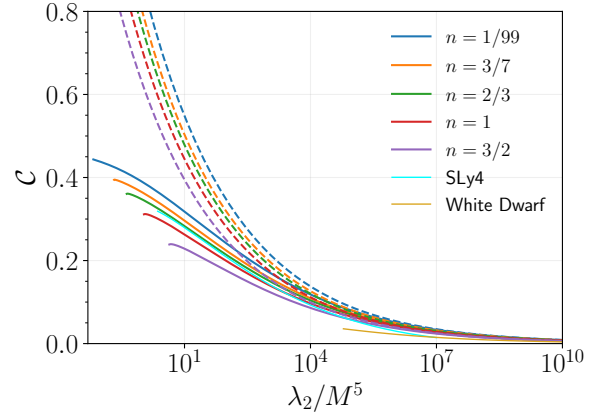


FIG. 5. An example of non-universal relation: the compactness C versus λ_2/M^5 . The dashed lines are the Newtonian results, and the solid lines are the results using GR. The results of NSs (SLy4) and white dwarfs are also plotted for comparison. Notice that the compactness of the Newtonian polytropic star extends to infinity.

tidal Love numbers for the 8 planets and some of their moons. While some moment of inertia factors and tidal Love numbers are not directly measured, they are theoretically inferred from models based on the current best understanding of these celestial objects. These models are used for comparison, as they are considered significantly more reliable than the simplistic model of spherical polytropic stars.

In Fig. 6, we depict the data for the moment of inertia and tidal Love number of the celestial objects listed in Table I, alongside the theoretical line of Eq. (42). The trend of the data aligns well with the theoretical line, particularly for planets. A linear regression of the data in the logarithmic scale yields:

$$\log_{10} \left(\frac{I}{M^3} \right) = 0.412 \log_{10} \left(\frac{\lambda_2}{M^5} \right) - 0.803, \quad (43)$$

TABLE I. Measured or theoretically calculated values of the moment of inertia and the tidal Love number for the planets and moons in the solar system.

Object	M [10^{22} kg]	R [10^6 m]	$I/(MR^2)$	k_2	Ref.
Mercury	33.0	2.440	0.333	0.464	[38, 39]
Venus	4.87×10^2	6.052	0.337	0.295	[40, 41]
Earth	5.97×10^2	6.378	0.331	0.301	[42, 43]
Mars	64.2	3.396	0.364	0.169	[44, 45]
Jupiter	1.90×10^5	71.49	0.276	0.535	[46, 47]
Saturn	5.68×10^4	60.27	0.22	0.379	[48, 49]
Uranus	8.68×10^3	25.56	0.23	0.319	[50, 51]
Neptune	1.02×10^4	24.76	0.23	0.29	[50, 52]
Moon	7.35	1.737	0.393	0.0242	[53, 54]
Ceres	9.47×10^{-2}	0.475	0.36	1.33	[55, 56]
Io	8.93	1.822	0.377	0.09	[57, 58]
Europa	4.80	1.561	0.355	0.24	[59, 60]
Ganymede	14.8	2.631	0.311	0.45	[59, 61]
Callisto	10.8	2.410	0.355	0.33	[61, 62]
Titan	13.5	2.576	0.341	0.62	[63, 64]
Enceladus	1.08×10^{-2}	0.190	0.335	0.02	[65]
Rhea	0.231	0.7644	0.391	1.42	[66]

with a R-Squared value of 0.984. The slope 0.412 is slightly greater than the theoretical value $2/5$. This is likely because the planets and the moons are slightly oblate due to their rotations or tides from nearby bodies, so they have larger moments of inertia than spherical bodies of the same masses.

III. SUMMARY

We have numerically calculated the moment of inertia (I) and the tidal Love number (k_2) for polytropic stars in both Newtonian gravity and GR. The I-Love relation varies within 1 % for different polytropic indices in Newtonian gravity and within 10 % for different polytropic indices in GR. The results explicitly demonstrate that the I-Love universal relation not only exists for compact stars but also exists for Newtonian stars.

We have also computed the moment of inertia and the tidal Love number for realistic NSs and white dwarfs to compare with the polytropic stars. We find that the I-Love relation of

the realistic NSs falls within 1 % of the I-Love relation of the $n \rightarrow 0$ polytropic case. For white dwarfs, their I-Love relation has a 10 % discrepancy away from the $n \rightarrow 0$ polytropic case when comparing to the GR solution; surprisingly, the I-Love relation for white dwarfs agrees better with the Newtonian result.

Finally, we have collected measured and theoretically inferred data of the moment of inertia and the tidal Love number for 17 celestial bodies in our solar system to check the I-Love universal relation obtained for polytropic stars. The trend of the data follows the theoretical line well. The slope of the best-fit line of the data deviates from the theoretical value $2/5$ by only 3 %, showing the adequacy of the theoretical I-Love universal relation in describing real planets and moons. Therefore, the I-Love universal relation provides a valuable tool for exploring exoplanets. Especially when combined with the Darwin–Radau equation [67], one can compute the moment of inertia and the tidal Love number of the exoplanet if its mass, spin frequency, equatorial radius, and polar radius are known. The moment of inertia and the tidal Love

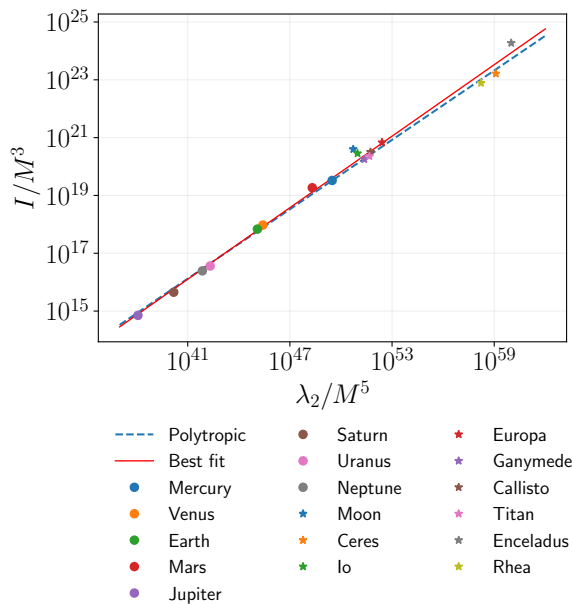


FIG. 6. The theoretical I-Love universal relation checked against the measurements of the solar-system celestial bodies.

number are closely related to the interior structure and compositions of the planet. Knowing them helps build detailed models of the exoplanet and thus understand it better.

ACKNOWLEDGMENTS

This work was supported by the China Postdoctoral Science Foundation (2023M741999), and the high-performance computing cluster in the Astronomy Department of Tsinghua University.

Appendix A: Zero-temperature white dwarfs

Here we append numerical results on the tidal deformability and the moment of inertia of white dwarfs, using the EOS of the zero-temperature degenerated electron gas. The derivation of the EOS can be found, for example, in Refs. [28, 68, 69]; we write down the parameterized EOS directly for our use. The number density, the energy density, and the pressure of the zero-temperature degenerated electron gas are

$$n_e = \frac{m_e^3}{3\pi^2\hbar^3} x^3,$$

$$\epsilon_e = \frac{m_e^4}{8\pi^2\hbar^3} \left[x\sqrt{1+x^2}(1+2x^2) + \ln(\sqrt{1+x^2}-x) \right],$$

$$p_e = \frac{m_e^4}{8\pi^2\hbar^3} \left[x\sqrt{1+x^2} \left(\frac{2}{3}x^2 - 1 \right) - \ln(\sqrt{1+x^2}-x) \right] \quad (\text{A1})$$

where $x := \sqrt{(E_F/m_e)^2 - 1}$ with E_F the Fermi energy of the electron gas and m_e the electron mass. While the pressure in white dwarfs can be approximated as

$$p \approx p_e, \quad (\text{A2})$$

the energy density in white dwarfs must take the rest energy of the nuclei into account, namely

$$\epsilon \approx \rho_n + \epsilon_e = \mu_e m_H n_e + \epsilon_e, \quad (\text{A3})$$

where $\mu_e \approx 2$ is the mean molecular weight and $m_H = 1.660539 \times 10^{-27}$ kg is the atomic mass unit.

Using the same formulae as in Sec II B but with the EOS given by Eqs. (A2) and (A3), we have calculated the mass-radius relation, the tidal deformability, and the moment of inertia for white dwarfs. Figures 7 and 8 show the results. Then in Fig. 9, the same I-Love relation plot as in Fig 3 is shown, with the focus now on the white dwarfs and the vertical axis in linear scale.

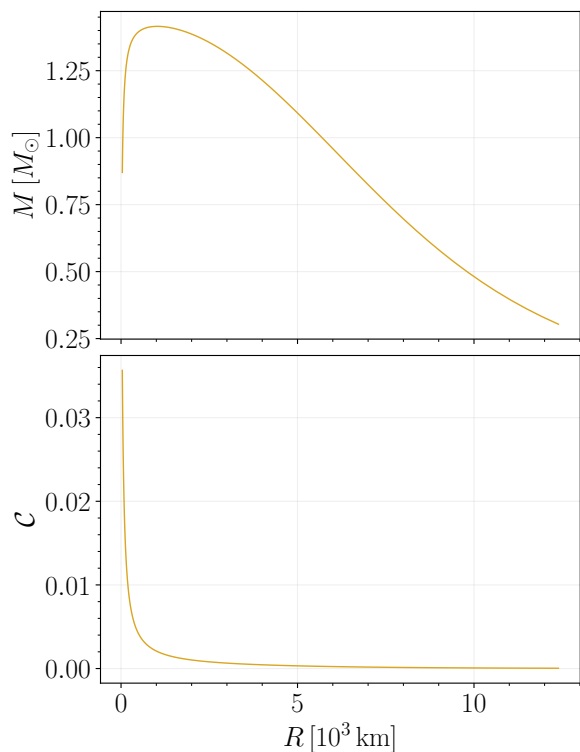


FIG. 7. Upper panel: the mass-radius relation of the zero-temperature white dwarfs. Lower panel: the compactness versus the radius of the zero-temperature white dwarfs.

[1] K. Yagi and N. Yunes, *Science* **341**, 365 (2013), arXiv:1302.4499 [gr-qc].

[2] K. Yagi and N. Yunes, *Phys. Rev. D* **88**, 023009 (2013),

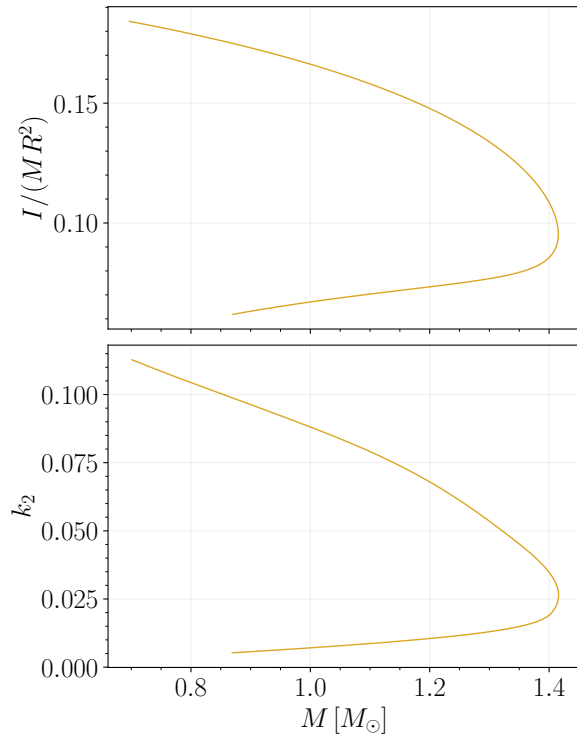


FIG. 8. Upper panel: the moment of inertia factor versus the mass of the zero-temperature white dwarfs. Lower panel: the tidal Love number versus the mass of the zero-temperature white dwarfs.

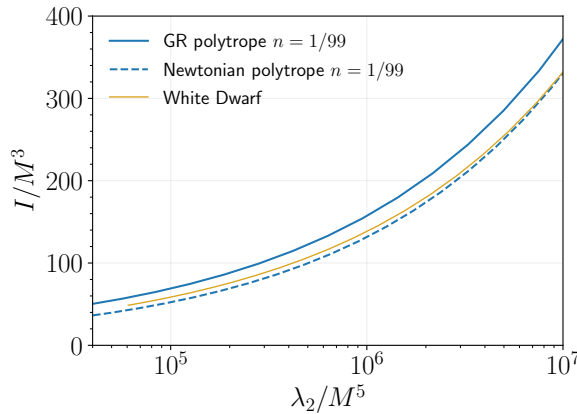


FIG. 9. The I-Love relation for the white dwarfs (red solid line) compared with the I-Love universal relation in Newtonian gravity (blue dashed line) and in GR (blue solid line).

- arXiv:1303.1528 [gr-qc].
- [3] K. Yagi, *Phys. Rev. D* **89**, 043011 (2014), [Erratum: *Phys.Rev.D* 96, 129904 (2017), Erratum: *Phys.Rev.D* 97, 129901 (2018)], arXiv:1311.0872 [gr-qc].
- [4] K. Yagi, K. Kyutoku, G. Pappas, N. Yunes, and T. A. Apostolatos, *Phys. Rev. D* **89**, 124013 (2014), arXiv:1403.6243 [gr-qc].
- [5] P. Pani, L. Gualtieri, and V. Ferrari, *Phys. Rev. D* **92**, 124003 (2015), arXiv:1509.02171 [gr-qc].
- [6] T. Delsate, *Phys. Rev. D* **92**, 124001 (2015), arXiv:1504.07335

- [gr-qc].
- [7] K. Yagi and N. Yunes, *Phys. Rept.* **681**, 1 (2017), arXiv:1608.02582 [gr-qc].
- [8] T. K. Chan, Y. H. Sham, P. T. Leung, and L. M. Lin, *Phys. Rev. D* **90**, 124023 (2014), arXiv:1408.3789 [gr-qc].
- [9] C. Chirenti, G. H. de Souza, and W. Kastaun, *Phys. Rev. D* **91**, 044034 (2015), arXiv:1501.02970 [gr-qc].
- [10] D. D. Doneva and K. D. Kokkotas, *Phys. Rev. D* **92**, 124004 (2015), arXiv:1507.06606 [astro-ph.SR].
- [11] A. Maselli, V. Cardoso, V. Ferrari, L. Gualtieri, and P. Pani, *Phys. Rev. D* **88**, 023007 (2013), arXiv:1304.2052 [gr-qc].
- [12] J. D. Bekenstein, *Phys. Rev. D* **51**, R6608 (1995).
- [13] A. Taylor, K. Yagi, and P. L. Arras, *Mon. Not. Roy. Astron. Soc.* **492**, 978 (2020), arXiv:1912.09557 [gr-qc].
- [14] K. Chen and L.-M. Lin, *Phys. Rev. D* **108**, 064007 (2023), arXiv:2307.01598 [gr-qc].
- [15] H. O. Silva, C. F. B. Macedo, E. Berti, and L. C. B. Crispino, *Class. Quant. Grav.* **32**, 145008 (2015), arXiv:1411.6286 [gr-qc].
- [16] K. Yagi and N. Yunes, *Phys. Rev. D* **91**, 123008 (2015), arXiv:1503.02726 [gr-qc].
- [17] G. Martinon, A. Maselli, L. Gualtieri, and V. Ferrari, *Phys. Rev. D* **90**, 064026 (2014), arXiv:1406.7661 [gr-qc].
- [18] C.-H. Yeung, L.-M. Lin, N. Andersson, and G. Comer, *Universe* **7**, 111 (2021), arXiv:2105.00798 [astro-ph.HE].
- [19] P. Laskos-Patkos, P. S. Koliogiannis, A. Kanakis-Pegios, and C. C. Moustakidis, *HNPS Adv. Nucl. Phys.* **29**, 94 (2023).
- [20] V. Guedes, S. Y. Lau, C. Chirenti, and K. Yagi, *Phys. Rev. D* **109**, 083040 (2024), arXiv:2402.10868 [astro-ph.HE].
- [21] D. D. Doneva and G. Pappas, *Astrophys. Space Sci. Libr.* **457**, 737 (2018), arXiv:1709.08046 [gr-qc].
- [22] T. Gupta, B. Majumder, K. Yagi, and N. Yunes, *Class. Quant. Grav.* **35**, 025009 (2018), arXiv:1710.07862 [gr-qc].
- [23] Z. Hu, Y. Gao, R. Xu, and L. Shao, *Phys. Rev. D* **104**, 104014 (2021), arXiv:2109.13453 [gr-qc].
- [24] R. Xu, Y. Gao, and L. Shao, *Phys. Rev. D* **105**, 024003 (2022), arXiv:2111.06561 [gr-qc].
- [25] H. O. Silva, J. Sakstein, L. Gualtieri, T. P. Sotiriou, and E. Berti, *Phys. Rev. Lett.* **120**, 131104 (2018), arXiv:1711.02080 [gr-qc].
- [26] D. D. Doneva and S. S. Yazadjiev, *Phys. Rev. Lett.* **120**, 131103 (2018), arXiv:1711.01187 [gr-qc].
- [27] G. Antoniou, A. Bakopoulos, and P. Kanti, *Phys. Rev. Lett.* **120**, 131102 (2018), arXiv:1711.03390 [hep-th].
- [28] E. Poisson and C. M. Will, *Gravity: Newtonian, Post-Newtonian, Relativistic* (Cambridge University Press, Cambridge, England, 2014).
- [29] K. S. Thorne, *Rev. Mod. Phys.* **52**, 299 (1980).
- [30] J. B. Hartle, *Astrophys. J.* **150**, 1005 (1967).
- [31] T. Hinderer, *Astrophys. J.* **677**, 1216 (2008), [Erratum: *Astrophys.J.* 697, 964 (2009)], arXiv:0711.2420 [astro-ph].
- [32] T. Damour and A. Nagar, *Phys. Rev. D* **80**, 084035 (2009), arXiv:0906.0096 [gr-qc].
- [33] T. Binnington and E. Poisson, *Phys. Rev. D* **80**, 084018 (2009), arXiv:0906.1366 [gr-qc].
- [34] T. Regge and J. A. Wheeler, *Phys. Rev.* **108**, 1063 (1957).
- [35] N. Andersson and G. L. Comer, *Living Rev. Rel.* **10**, 1 (2007), arXiv:gr-qc/0605010.
- [36] E. Chabanat, J. Meyer, P. Bonche, R. Schaeffer, and P. Haensel, *Nucl. Phys. A* **627**, 710 (1997).
- [37] E. Chabanat, P. Bonche, P. Haensel, J. Meyer, and R. Schaeffer, *Nucl. Phys. A* **635**, 231 (1998), [Erratum: *Nucl.Phys.A* 643, 441–441 (1998)].
- [38] A. K. Verma and J.-L. Margot, *Journal of Geophysical Research (Planets)* **121**, 1627 (2016), arXiv:1608.01360 [astro-ph.EP].

- [39] A. Genova, S. Goossens, E. Mazarico, F. G. Lemoine, G. A. Neumann, W. Kuang, T. J. Sabaka, S. A. Hauck, D. E. Smith, S. C. Solomon, and M. T. Zuber, *Geophysical Research Letters* **46**, 3625 (2019).
- [40] A. S. Konopliv and C. F. Yoder, *Geophysical Research Letters* **23**, 1857 (1996).
- [41] J.-L. Margot, D. B. Campbell, J. D. Giorgini, J. S. Jao, L. G. Snedeker, F. D. Ghigo, and A. Bonsall, *Nature Astronomy* **5**, 676 (2021), [arXiv:2103.01504 \[astro-ph.EP\]](https://arxiv.org/abs/2103.01504).
- [42] J. G. Williams, *Astronomical Journal* **108**, 711 (1994).
- [43] M. Jagoda and M. Rutkowska, *Acta Geodaetica et Geophysica* **51**, 493 (2016).
- [44] A. S. Konopliv, S. W. Asmar, W. M. Folkner, Ö. Karatekin, D. C. Nunes, S. E. Smrekar, C. F. Yoder, and M. T. Zuber, *Icarus* **211**, 401 (2011).
- [45] A. S. Konopliv, R. S. Park, A. Rivoldini, R.-M. Baland, S. Le Maistre, T. Van Hoolst, M. Yseboodt, and V. Dehant, *Geophysical Research Letters* **47**, e90568 (2020).
- [46] S. M. Wahl, W. B. Hubbard, and B. Militzer, *Astrophysical Journal* **831**, 14 (2016).
- [47] D. Ni, *Astronomy and Astrophysics* **613**, A32 (2018).
- [48] J. J. Fortney, R. Helled, N. Nettelmann, D. J. Stevenson, M. S. Marley, W. B. Hubbard, and L. Iess, in *Saturn in the 21st Century*, edited by K. H. Baines, F. M. Flasar, N. Krupp, and T. Stallard (2018) pp. 44–68.
- [49] V. Lainey, J. W. Dewberry, J. Fuller, N. Cooper, N. Rambaux, and Q. Zhang, *Astronomy and Astrophysics* **684**, L3 (2024).
- [50] C. F. Yoder, in *Global Earth Physics: A Handbook of Physical Constants*, edited by T. J. Ahrens (1995) p. 1.
- [51] L. Stixrude, S. Baroni, and F. Grasselli, *Planetary Science Journal* **2**, 222 (2021).
- [52] D. A. James and L. Stixrude, *Space Science Reviews* **220**, 21 (2024).
- [53] J. G. Williams, X. X. Newhall, and J. O. Dickey, *Planetary Space Science* **44**, 1077 (1996).
- [54] J. G. Williams, A. S. Konopliv, D. H. Boggs, R. S. Park, D.-N. Yuan, F. G. Lemoine, S. Goossens, E. Mazarico, F. Nimmo, R. C. Weber, S. W. Asmar, H. J. Melosh, G. A. Neumann, R. J. Phillips, D. E. Smith, S. C. Solomon, M. M. Watkins, M. A. Wiczorek, J. C. Andrews-Hanna, J. W. Head, W. S. Kiefer, I. Matsuyama, P. J. McGovern, G. J. Taylor, and M. T. Zuber, *Journal of Geophysical Research (Planets)* **119**, 1546 (2014).
- [55] T. B. McCord and C. Sotin, *Journal of Geophysical Research (Planets)* **110**, E05009 (2005).
- [56] X. Mao and W. B. McKinnon, *Icarus* **299**, 430 (2018).
- [57] V. N. Zharkov and T. V. Gudkova, *Planetary Space Science* **58**, 1381 (2010).
- [58] M. Kervazo, G. Tobie, G. Choblet, C. Dumoulin, and M. Běhouňková, *Icarus* **373**, 114737 (2022).
- [59] G. Schubert, J. D. Anderson, T. Spohn, and W. B. McKinnon, in *Jupiter. The Planet, Satellites and Magnetosphere*, Vol. 1, edited by F. Bagenal, T. E. Dowling, and W. B. McKinnon (2004) pp. 281–306.
- [60] F. Petricca, S. Tharimena, D. Melini, G. Spada, A. Bagheri, M. J. Styczinski, and S. D. Vance, *Icarus* **417**, 116120 (2024).
- [61] T. Van Hoolst, G. Tobie, C. Vallat, N. Altobelli, L. Bruzzone, H. Cao, D. Dirkx, A. Genova, H. Hussmann, L. Iess, J. Kimura, K. Khurana, A. Lucchetti, G. Mitri, W. Moore, J. Saur, A. Stark, A. Vorbürger, M. Wiczorek, A. Abouan, J. Bergman, F. Bovolo, D. Breuer, P. Cappuccio, L. Carrer, B. Ceconi, G. Choblet, F. De Marchi, M. Fayolle, A. Fienga, Y. Futaana, E. Hauber, W. Kofman, A. Kumamoto, V. Lainey, P. Molyneux, O. Mousis, J. Plaut, W. Puccio, K. Retherford, L. Roth, B. Seignovert, G. Steinbrügge, S. Thakur, P. Tortora, F. Tosi, M. Zannoni, S. Barabash, M. Dougherty, R. Gladstone, L. I. Gurvits, P. Hartogh, P. Palumbo, F. Poulet, J.-E. Wahlund, O. Grasset, and O. Witasse, *Space Science Reviews* **220**, 54 (2024).
- [62] W. B. Moore and G. Schubert, *Icarus* **166**, 223 (2003).
- [63] L. Iess, R. A. Jacobson, M. Ducci, D. J. Stevenson, J. I. Lunine, J. W. Armstrong, S. W. Asmar, P. Racioppa, N. J. Rappaport, and P. Tortora, *Science* **337**, 457 (2012).
- [64] D. Durante, D. J. Hemingway, P. Racioppa, L. Iess, and D. J. Stevenson, *Icarus* **326**, 123 (2019).
- [65] A. Genova, M. Parisi, A. M. Gargiulo, F. Petricca, S. Andolfo, T. Torrini, E. Del Vecchio, C. R. Glein, M. L. Cable, C. B. Phillips, N. E. Bradley, R. L. Restrepo, D. M. Mages, A. Babuscia, and J. I. Lunine, *Planetary Science Journal* **5**, 40 (2024).
- [66] J. D. Anderson and G. Schubert, *Geophysical Research Letters* **34**, L02202 (2007).
- [67] G. Bourda and N. Capitaine, *Astron. Astrophys.* **428**, 691 (2004), [arXiv:0711.4575 \[astro-ph\]](https://arxiv.org/abs/0711.4575).
- [68] S. L. Shapiro and S. A. Teukolsky, *Black holes, white dwarfs, and neutron stars: The physics of compact objects* (1983).
- [69] S. Chandrasekhar, *An Introduction to the Study of Stellar Structure* (Dover Publications, 2010).